

Sensitivity analysis of an inverse procedure for determination of elastic coefficients for strong anisotropy

Hanuš Seiner^{a,b}, Michal Landa^{b,*}

^a Department of Materials, CTU Faculty of Nuclear Sciences and Physical Engineering, Trojanova 13, 120 00 Prague 2, Czech Republic

^b Institute of Thermomechanics, Czech Academy of Sciences, Dolejškova 5, 182 00 Prague 8, Czech Republic

Received 18 January 2004; accepted 8 July 2004

Available online 9 August 2004

Abstract

The elastic coefficients of anisotropic solids are often evaluated from measurements of phase or group velocities of ultrasonic bulk waves by the usage of inverse optimizing procedures. This paper discusses the effects of various factors on such procedures results for transversely isotropic solids with considerably strong anisotropy. First, the inverse determination of all elastic coefficients of unidirectional CFRP composite is briefly outlined. Then the results of the optimization are treated as exact values and the sensitivity of the optimizing process versus main considered sources of inaccuracies is analyzed. Results of extensive simulations are presented to illustrate the effect of input data distortion, input data incompleteness, and geometrical conversion from experimentally obtained group velocities into corresponding phase velocities used as input data for the optimizing procedure. The paper takes note of how information about the elastic coefficients can be extracted from the different segments of the phase velocity surface. The stability versus input data distortion for inversion from group velocities and phase velocities is compared and the importance of reliable geometrical converting from group into phase velocities is illustrated. An novel method for geometrical conversion of distorted group velocity data into corresponding phase velocities based on affine combinations of low-order polynomials is presented and compared with piecewise or high-order polynomial fitting.

© 2004 Elsevier B.V. All rights reserved.

PACS: 43.35; 62.65

Keywords: Elastic anisotropy; Group velocity; Non-destructive evaluation; Inverse problem; Sensitivity analysis

1. Introduction

Measurement of ultrasonic phase or group velocities in various directions is one of the most common methods for examination of material anisotropic properties [1]. The experiment can be set up variously. Usually either the velocities of planar waves travelling through specimen immersed in water or oil are measured [2–6], or the point-source/point-receiver techniques are applied

[7–13], where the wave arrivals from a point source are in situ detected by miniature piezoelectric transducers or laser interferometry and group velocities in various direction are thus obtained.

As it results from the completely described theory of bulk wave propagation [14–17], the phase velocities v_φ are related to the elastic coefficients c_{ijkl} nonlinearly via the determinant of the Christoffel equation

$$\Omega(\omega, \mathbf{k}) = \det(n_j c_{ijkl} n_l - \delta_{ik} \rho v_\varphi^2), \quad (1)$$

where ρ is the mass density, $\mathbf{k} = k \cdot \mathbf{n}$ is the wave vector and ω the angular frequency of the considered planar harmonic wave. However, the energy carried by the wave travels through the anisotropic sample with the group velocity, which, in general, differs from the phase

* Corresponding author. Tel.: +4202 6605 3672; fax: +4202 8658 4695.

E-mail address: ml@it.cas.cz (M. Landa).

velocity in both the magnitude and the direction and its relation with the elastic coefficients is even more complex. Although the explicit dependence of the group velocity vector on the direction \mathbf{n} normal to the phase fronts can be derived in some particular cases [8,15,18], evaluation of the group velocity magnitude for given direction is usually more difficult.

Corresponding group and phase velocities of each mode are geometrically related by polar reciprocity between the ray surface (plot of group velocity magnitude versus its direction) and the slowness surface (plot of reciprocal phase velocity $1/v_\phi$ versus normal to phase fronts \mathbf{n}), which results in equation

$$\frac{\mathbf{n} \cdot \mathbf{v}_G}{v_\phi} = 1. \quad (2)$$

Via this equation, the group velocities can often be converted into corresponding phase velocities (e.g. [8]), and both the measurements of phase and group velocities thus lead to similar inverse optimizing problem. The sought elastic coefficients are to be found by minimization of the sum

$$Q = \sum_{n=1}^N (v_\phi(c_{ij}, \mathbf{n}_n) - v_\phi^{\text{ex}}(\mathbf{n}_n))^2 \rightarrow \min_{c_{ij}}, \quad (3)$$

where the superscript ‘ex’ denotes the experimentally obtained value. Because each evaluation of such sum consists of an eigenvalue problem solution, the simplex method seems to be the most suitable optimizing technique for this problem since this method requires a minimum number of sum evaluations [19]. As usual for similar inverse problems, the numerical procedure should always tend to converge to some values. The sum Q , treated as a function of sought elastic coefficients c_{ij} for a given set of experimental velocities v_ϕ^{ex} , may contain various local minima differing from the correct optimum values. The correctness of numerically obtained elastic coefficients is most widely controlled by visual agreement between input experimental data and normal surfaces (plot of phase velocity magnitude versus \mathbf{n}) evaluated for optimized coefficients. As will be illustrated later, such agreement may not guarantee the correctness of optimized values, especially when the input data insufficiently cover the corresponding normal surface.

In this paper, the stability and accuracy of such simplex optimizing algorithm is demonstrated for transversely isotropic materials. Among the materials with this type of symmetry is belong the unidirectional fibrous composite materials, many biological materials such as bones [20] and some single crystals, e.g. zinc. Such materials exhibit rotational invariance in all mechanical properties about one symmetry axis, usually denoted x_3 . Anisotropic elastic behavior of transversely isotropic media is characterized by five independent elastic coefficients

$$c = \begin{pmatrix} c_{11} & c_{12} & c_{13} & 0 & 0 & 0 \\ c_{12} & c_{11} & c_{13} & 0 & 0 & 0 \\ c_{13} & c_{13} & c_{33} & 0 & 0 & 0 \\ 0 & 0 & 0 & c_{44} & 0 & 0 \\ 0 & 0 & 0 & 0 & c_{44} & 0 \\ 0 & 0 & 0 & 0 & 0 & \frac{c_{11}-c_{12}}{2} \end{pmatrix}.$$

The plane normal to the x_3 axis is the isotropic symmetry plane x_1x_2 . All directions including the same angle with the plane x_1x_2 are thus equivalent, and each set of such crystallographically equivalent directions can be represented only by one angle—the angle ϑ contained with the principal isotropic plane x_1x_2 . The symmetry axis x_3 corresponds, thus, to $\vartheta = 90^\circ$ and each direction in principal plane x_1x_2 to $\vartheta = 0^\circ$. To distinguish the group velocity directions, the angle of similar meaning as ϑ but belonging to group velocities will be denoted ξ instead of ϑ . The angles ϑ and ξ of corresponding phase and group velocities coincide in the principal isotropic plane and in the rotational axis x_3 .

Ultrasonic waves in transversely isotropic media can generally propagate in three modes. The mode with polarization vector closest to the direction of propagation is called quasi-longitudinal and will be denoted by qL. The slower modes are the quasi-transverse mode (qT) with polarization vector lying in the same symmetry plane as of the qL mode and the pure-transverse mode with polarization vector normal to the direction of propagation, which will be denoted by PT.

The transversal isotropy enables velocity measurements in all directions to be treated as located in one plane containing the symmetry axis. The five-dimensional optimization problem (3) for such materials can be recast as

$$Q = \sum_{n=1}^N (v_\phi(c_{ij}, \vartheta_n) - v_\phi^{\text{ex}}(\vartheta_n))^2 \rightarrow \min_{c_{ij}}, \quad (4)$$

where the indexes ij are taken from the set $ij \in \{11, 12, 13, 33, 44\}$.

Let us now describe such optimizing process for a unidirectional CFRP composite. First, the elastic coefficients will be determined from group velocities obtained by point-source/point-receiver technique. Then, the results will be thoroughly discussed in order to estimate the reliability of optimized results. As it follows from findings of Every and Sachse [21] or Chu and Rokhlin [22], the procedure’s sensitivity to various constants is significantly dependent not only on accuracy and completeness of the input data but also on class and proportion of considered material’s anisotropy. In addition, this paper statistically analyzes, how are the results influenced by a geometrical conversion of group velocities into corresponding phase velocities, which is one of the most important passages of the whole inverse process.

2. Determination of elastic coefficients of unidirectional CFRP composite

The elastic coefficients used for further simulations were obtained on a plate-shaped specimen (120 mm × 120 mm × 7.514 mm) made of unidirectional CFRP¹ composite with mass density $\rho = 1.514 \text{ g cm}^{-3}$. The fiber direction has been considered to be parallel to the specimens surfaces.

The experimental apparatus (for more details, see [12,13]) consisted of two miniature piezoelectric transducers fixed on opposite sides of the specimen and of one moving point-like source, implemented by impacts of focused laser beam, as outlined in Fig. 1.

Due to transversal isotropy, the waves propagating from the source to both transducers can be treated as lying in one symmetry plane containing the rotational axis. For the source moving on the circle with radius $r = 20 \text{ mm}$ equidistantly by an angular step 1° , 91 various waveforms were obtained on each of transducers in each quadrant of such principal plane.

On the same specimen, the pulse-echo measurements in direction normal to the fibers were performed, which resulted in getting of accurate values of velocities of all three modes. From these velocities, the coefficients c_{11} , c_{12} and c_{44} can be conveniently evaluated, using the well known explicit formulae [9]. The knowledge of these coefficients enables the dimension of the solved optimizing problem (4) to be reduced from five to two, (e.g. [23]). The coefficients c_{13} and c_{33} remained to be determined by solving a two-dimensional optimizing problem

$$Q = \sum_{n=1}^N (v_\varphi(c_{ij}, \vartheta_n) - v_\varphi^{\text{ex}}(\vartheta_n))^2 \rightarrow \min_{c_{13}, c_{33}}. \quad (5)$$

Because of the complicated shape of the signals measured on the transducers, which hindered the identification of wave arrivals corresponding to particular modes, except the fastest qL-mode, the following successive procedure was employed:

1. From the first wave arrival on the detectors, the velocities of the fastest (qL) mode were obtained.
2. The obtained group velocities were geometrically converted into phase velocities.
3. The obtained qL phase velocities were used as an input for the two-dimensional optimizing procedure. This issue consisting in optimal determination of elastic coefficients form the quasi-longitudinal phase velocities was exhaustively analyzed by Every and

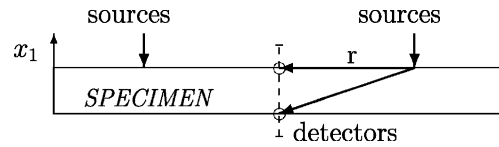


Fig. 1. Experimental setup for measurement of group velocities in thick CFRP composite plate.

Sachse in [21] for weak anisotropy ($|c_{AB} - c_{AB}^0| \leq \varepsilon c_{11}^0$ for all $A, B \in \{1, \dots, 6\}$, where $\varepsilon \ll 1$ is a small positive number and c_{AB}^0 a matrix of isotropic elastic coefficients) employing the perturbation method. For such materials, the phase velocities of qL waves can be approximately evaluated as [8]

$$v_\varphi^{\text{qL}} = \sqrt{(c_{11}n_1^4 + c_{33}n_3^4 + 2(c_{13} + 2c_{44})n_1^2n_3^2)/\rho} \quad (6)$$

and these velocities are, thus, obviously dependent on c_{11} , c_{33} and $c_{13} + 2c_{44}$. So for c_{11} taken as known from the pulse-echo measurements in direction x_1 , the minimum (4) should be sought with respect to c_{33} and $c_{13} + 2c_{44}$. One of the necessary conditions for weak anisotropy is that $c_{11} \approx c_{22} \approx c_{33}$, which obviously not valid for CFRP composite materials. However, some sensitivity of qL velocities to the combination $c_{13} + 2c_{44}$ remains even for moderate anisotropy (single crystal of zinc, $c_{11} \approx 2.5c_{33}$, [21]) and for strong anisotropy (graphite/epoxy composite, $c_{33} \approx 9.5c_{11}$, [22]). The sensitivity of qL velocities to individual coefficient c_{13} is amplified by increasing anisotropy, [7,22], so for the strong anisotropy, the coefficient c_{13} can be determined individually, especially when c_{44} is known (graphite/epoxy composite, $c_{33} \approx 9.1c_{11}$, [23]). For such materials, the evaluation of c_{13} by subtracting the known value of c_{44} (measured by a pulse-echo method in direction x_1) from the optimal value of combination $c_{13} + 2c_{44}$ is significantly less accurate than the two dimensional optimization with respect to c_{13} and c_{33} .

4. The ray surface of the qT-mode was constructed for the coefficients c_{ij} evaluated from the qL mode, and then the arrivals of the qT-mode were determined in some regions as the wave arrivals closest to this ray surface.
5. The obtained regions of qT-mode were geometrically converted into corresponding phase velocities used as the input for a new optimizing procedure, together with the previously used qL-velocities. This optimizing procedure was four-dimensional (ij were taken from the set $\{11, 13, 33, 44\}$) in order to compare the results from the direct pulse-echo method with those obtained by the point-source/point-receiver technique. This approach revealed a small deviation of the material properties from the rotational invariance about the fiber direction (in fact, the examined unidirectional composite seems to be insignificantly orthotropic).

¹ Unidirectional Carbon Fiber Reinforced Composite, prepreg Fibredux S913C-HTA-(12k)-5-40%, produced by La-Composite Letov ATG, 56 layers.

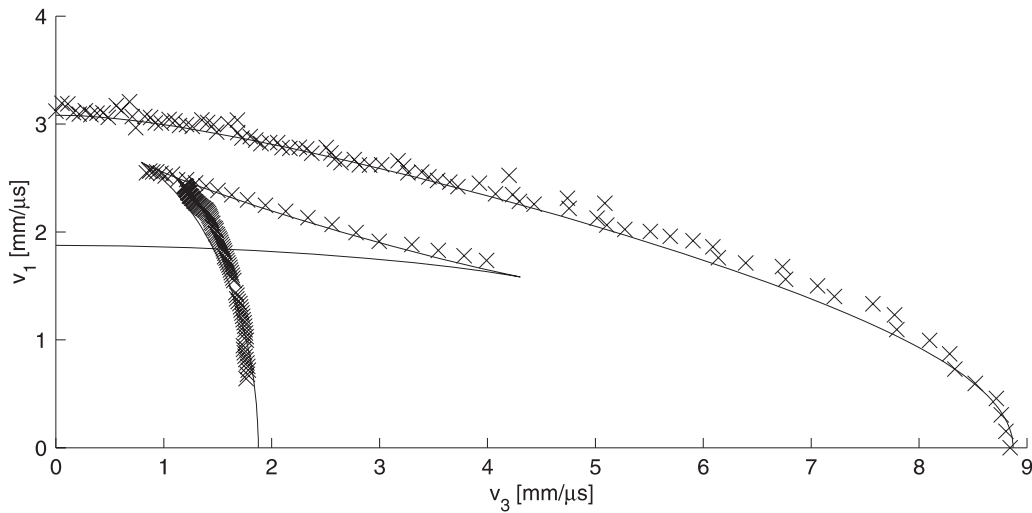


Fig. 2. Agreement between experimentally obtained group velocities (denoted by crosses) and ray surfaces evaluated for resultant elastic coefficients (solid lines) of the qL and qT modes.

The resultant elastic coefficients for considered transversal isotropy were evaluated by averaging those obtained from pulse echo measurements in direction normal to the specimen and those corresponding to propagation in the plane of the specimen obtained by inverse procedure from the point-source/point-receiver measurements, which resulted in $c_{11} = 14.4$ GPa, $c_{12} = 7.8$ GPa, $c_{13} = 6.7$ GPa, $c_{33} = 119.5$ GPa, $c_{44} = 5.3$ GPa [12,13]. The agreement between experimental input group velocity data and group velocity curves evaluated for the above listed coefficients is shown in Fig. 2.

3. Numerical analysis of the optimizing process

For following analysis, the above determined elastic coefficients will be treated as exact values (c_{ij}^{exact}). The stability of the whole optimizing process will be examined with respect to various possible sources of inaccuracies.

The sought minimum of the five-dimensional function (4) may be of various shapes, depending on how strongly the input set of velocities determines the particular elastic coefficient, as it is obvious in Fig. 3.

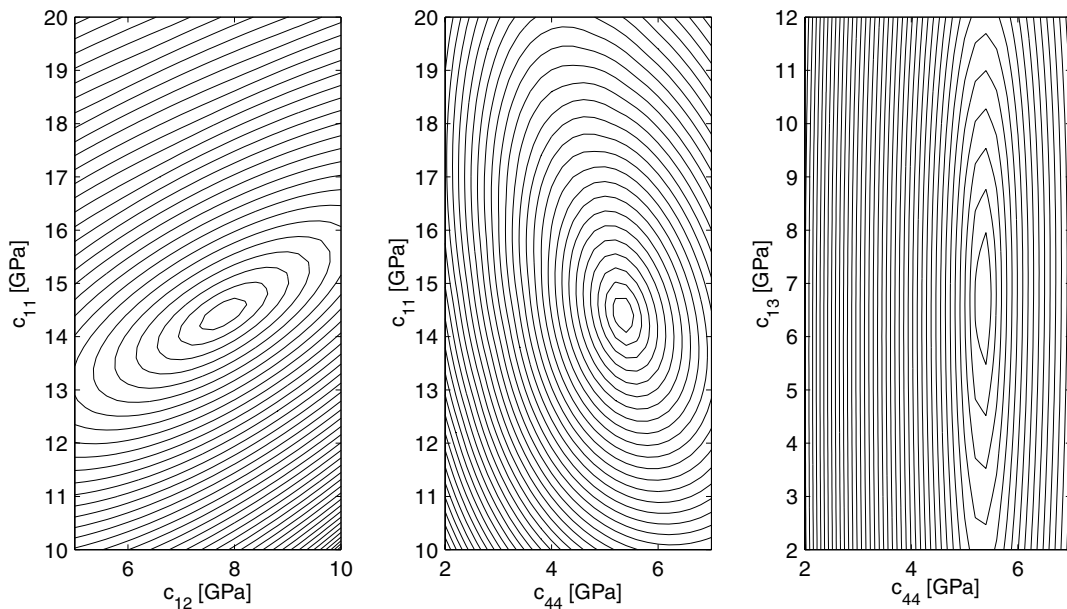


Fig. 3. Chosen contour plots of sought five-dimensional minimum of function Q_{ϕ} , as it is defined by 10 exact values of v_{ϕ} for each mode, covering equidistantly all modes.

To discuss the correctness of the optimizing procedure, appropriate measures for agreement must be defined between exact elastic coefficients (c_{ij}^{exact}) and elastic coefficients (c_{ij}^{output}) obtained as an output of some inverse algorithm. For the results of a single optimizing process (4) or (5), the measure

$$\delta c_{ij} \stackrel{\text{def.}}{=} \left| \left(c_{ij}^{\text{output}} - c_{ij}^{\text{exact}} \right) / c_{ij}^{\text{exact}} \right| \quad (7)$$

will be used. Within the sensitivity analyses, the inverse algorithms are applied several times on e.g. variously distorted experimental data and sets of output elastic coefficients ($c_{ij}^{\text{output}1, \dots, n}$) are obtained. Then the result should be treated statistically, represented by the differences between the mean and resultant values

$$\delta_{ij} = \frac{\bar{c}_{ij} - c_{ij}^{\text{exact}}}{c_{ij}^{\text{exact}}}, \quad \text{where } \bar{c}_{ij} = \frac{1}{n} \sum_{k=1}^n (c_{ij}^{\text{output}})^{(k)} \quad (8)$$

and by the relative standard deviations SD_{ij}/c_{ij} , where

$$SD_{ij} = \left(\frac{1}{n-1} \sum_{k=1}^n (c_{ij}^{(k)} - \bar{c}_{ij})^2 \right)^{1/2}. \quad (9)$$

Let us now discuss the influence of input data distortion, input data incompleteness and group velocity conversion on results of the optimizing process.

4. Input data distortion

As it is natural to any experimental data, the input velocities may be accidentally distorted about correct values. Such distortion will probably result in some loss of accuracy of an optimizing process [4,22,24]. To analyze, whether the input data distortion may significantly influence the optimization results, extensive simulations were performed.

The experimental data were expected to be normally distributed about correct values. For various data distortion ranging from distortion rate $\sigma = 1\%$ of v_φ (minimum distortion) to $\sigma = 3\%$ of v_φ (quite significant distortion, see Fig. 4), sets of distorted velocities were generated and those sets were then used as input data for optimization procedure (4). The optimization was repeated 30 times ($n = 30$ in Eqs. (8) and (9)). The input data for each repetition consisted of 10 values of each mode, covering the normal surfaces equidistantly by 10° step. It may serve as a basis for another more exhaustive statistical analysis whether the output values c_{ij} are normally distributed or have at least symmetrical distribution about correct values, but they will be treated so anyway. The relative standard deviations of output values are listed in Table 1.

Comparing the columns of this table, we can conclude that whereas the diagonal coefficients c_{11} , c_{33} , and c_{44} are of deviations comparable with input data

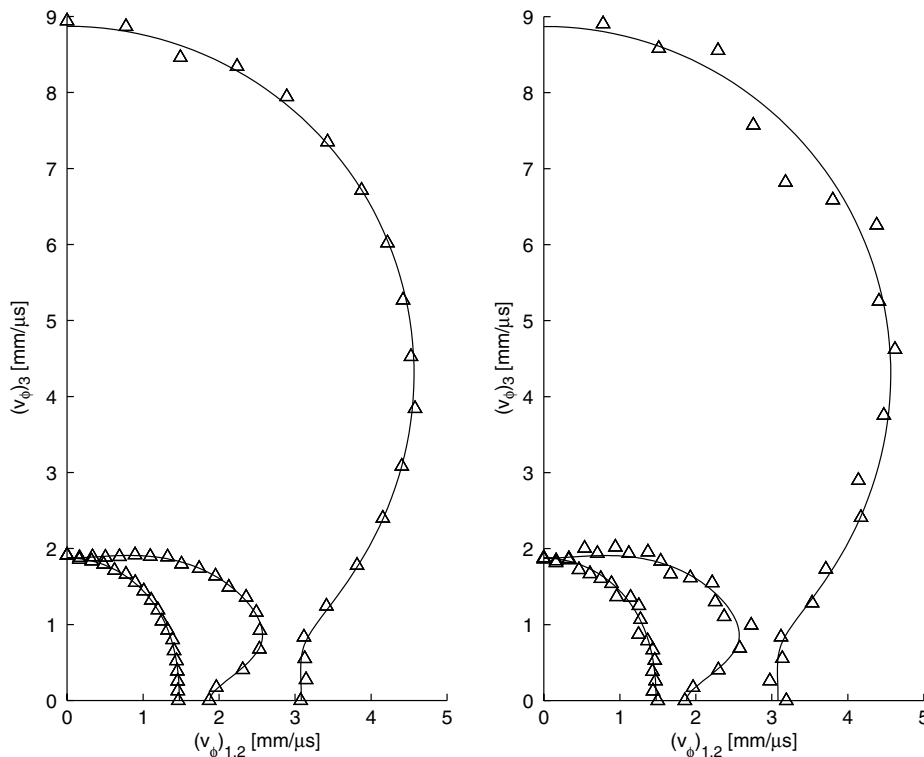


Fig. 4. Minimal ($\sigma = 1\%$ of v_φ) and significant ($\sigma = 3\%$ of v_φ) distortion of input velocities. Solid lines denote exact normal surfaces.

Table 1

Dependence of relative standard deviations of output elastic coefficients on input data distortion

Distortion (%)	SD ₁₁ /c ₁₁ (%)	SD ₁₂ /c ₁₂ (%)	SD ₁₃ /c ₁₃ (%)	SD ₃₃ /c ₃₃ (%)	SD ₄₄ /c ₄₄ (%)
1	1.29	2.88	10.61	0.90	0.75
2	2.40	4.84	27.14	1.89	1.75
3	3.84	7.35	31.01	2.78	2.49

Table 2

Effect of mode omission on output values of elastic coefficients

Mode omitted	δc ₁₁ (%)	δc ₁₂ (%)	δc ₁₃ (%)	δc ₃₃ (%)	δc ₄₄ (%)
PT	0.02	51.71	0.14	0.01	0.00
qT	0.02	0.01	0.08	0.01	0.03
qL	8.06	14.70	>100	26.49	0.68

distortions, the remaining coefficients c_{12} and c_{13} , especially the second one, are much more sensitive to input data distortion. This effect can be explained by starting the simulation for accurate input data once again with omitting one of the propagation modes, see Table 2.

This table implies that the coefficient c_{13} is significantly related to velocities of the quasi-longitudinal mode. Its value is thus optimized to fit preferentially one third of all input data, which multiplies the effect of data distortion. Such conclusion cannot be estimated from explicit formulae for phase velocities in transversely isotropic solids as derived e.g. in [1], from which the qT and qL modes seem to be equivalent to each other. However, only the values of the qL mode are insufficient for stable determination of coefficient c_{13} as well, as will be illustrated in next section.

As far as the coefficient c_{12} is concerned, it has been taken into account that both the qL and qT velocities are independent on this coefficient [1] and its determination is thus related only with values of the PT mode. The loss of accuracy for this coefficient when the qL mode is omitted may be explained from the explicit relation for PT phase velocities

$$\rho v_{\varphi}^{\text{PT}} = \sqrt{c_{66} \cos^2 \vartheta + c_{44} \sin^2 \vartheta}, \quad \text{where } c_{66} = \frac{c_{11} - c_{12}}{2}. \quad (10)$$

We can conclude, that every inaccuracy in determination of coefficients c_{11} and/or c_{44} may influence the accuracy of resultant coefficient c_{12} .

Naturally, it can be supposed that the effect of input data distortion is strongly dependent on the number of input data and may be very specific for each particular case of symmetry and for every particular material.

5. Input data incompleteness

The described simulation with mode omission leads us to an other possible source of the inverse algorithms

failure. The omission of some normal surface regions may lead to a total loss of stability for some elastic coefficients.

When all three modes are covered, the algorithm remains stable, even though some range of directions is omitted. The simulation was performed for omission of regions $\vartheta \in \langle 60^\circ; 90^\circ \rangle$, $\vartheta \in \langle 30^\circ; 60^\circ \rangle$ and $\vartheta \in \langle 0^\circ; 30^\circ \rangle$, resulting in no significant loss of stability or accuracy of the optimizing process.

Unfortunately, the arrivals of transversal modes (qT and PT) may be very difficult to detect, and the loss of stability due to mode omission (as outlined in Table 2) becomes crucial.

However, as utilized in the first section, this problem can be conveniently circumvented, when accurate measurements of all modes in any direction lying in the principal plane are available. From such pulse-echo measurements [12,23], that enable one to distinguish between qT and PT modes from their polarization directions, the elastic coefficients c_{11} , c_{12} and c_{44} can be directly determined, which reduces the dimension of optimizing procedure (4) from five to two. Then the most easily identifiable qL-mode is sufficient for inverse evaluation of remaining coefficients c_{13} and c_{33} .

Let us now examine, how such simplification influences the stability of the inverse algorithm. Similar simulation as for the all three modes in previous sections were performed, again repeating the optimizing process 30 times for each level of data distortion. To make the results comparable with those of Table 1, the same number of input data (30 values) has been used. Relative standard deviations resulting from this simulation are listed in Table 3. The results in Tables 1 and 3 are very close to each other, the stability of inversion process is, thus, due to considered simplification neither impaired nor improved. The coefficient c_{13} still remains to be significantly influenced by input data distortion.

In Fig. 5, another kind of input data incompleteness is examined. As demonstrated above, different modes of propagation are differently suitable for inverse determination of a given elastic coefficient. In a similar way, various regions of the normal surface contain various information about the elastic coefficients.

This figure presents results of two-dimensional inverse procedures (c_{13} and c_{33} determined for remaining coefficients taken as known) applied to various segments of the qL phase velocity curve. The same number of ex-

Table 3

Dependence of relative standard deviations of output elastic coefficients on distortion of input qL data

Distortion	SD ₁₃ /c ₁₃ (%)	SD ₃₃ /c ₃₃ (%)
1	10.04	0.50
2	25.48	1.01
3	33.27	1.52

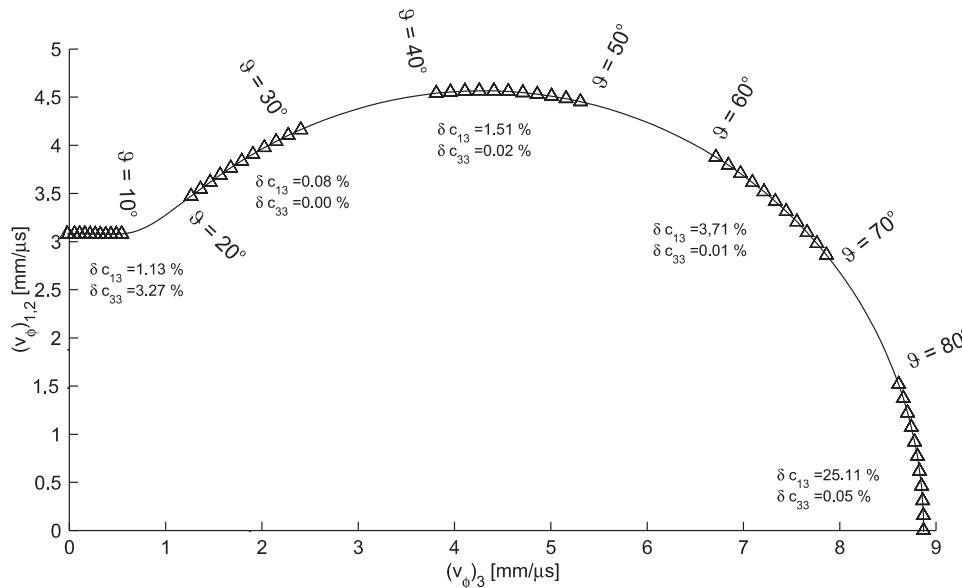


Fig. 5. Accuracy of coefficients c_{13} and c_{33} resulting from the same number of theoretically calculated qL phase velocities covering different segments of the normal surface.

actly evaluated input phase velocities (i.e. input data with no distortion) covering the same range of angles (10°) results in different accuracy of the output values. The results might suggest in which directions the phase velocities should be measured to obtain the most accurate output of the optimizing procedure.

Unsurprisingly, the velocities in directions close to the isotropic plane x_1x_2 contain weaker information about the coefficient c_{33} .

To observe the accuracy of c_{13} along the curve appears to be more important. Best results are obtained close to the isotropic plane, especially for $\vartheta \in \langle 20^\circ; 30^\circ \rangle$. That might be the region where the curve is most sensitively dependent on the individual coefficient c_{13} .

Such conclusion is somehow in agreement with findings of Minachi et al. in [23], where the inversion was done from group velocities corresponding to phase velocities lying mostly straight in this interval. That resulted in very accurate determination of the coefficient c_{13} (compare with [22]).

Generally, the effect of input data incompleteness may vary from insignificant distortion of output values to a crucial loss of stability. For each kind of material, similar simulation must be done to predict possible sources of inversion failure.

6. Group velocity conversion

As mentioned in the introduction and employed in the first section, the ray surface $v_G(\mathbf{n})$ and the slowness surface $\frac{1}{v_\varphi}(\mathbf{n})$ are polar reciprocal to each other. The normal surface $v_\varphi(\mathbf{n})$ can be thus proved to be the tangent

plane to the ray surface, whereas the ray surface is the foot-point (or pedal) surface to the normal surface [16]. Consequently, from the knowledge or approximate guess of direction normal to the ray surface, the corresponding point of the normal surface can be geometrically constructed, as described in [14–17]. The determination of normal direction becomes the most important stage of whole velocity conversion, especially when the input experimental ray surface is too distorted or otherwise unsuitable for direct numerical treatment. Then the ray surface must be fitted first by appropriate smooth (or piecewise smooth) function of known analytical form, which allows an analytical expression of normal direction in considered points.

The simplest and most widely used fitting functions are naturally the polynomials, usually approximating the magnitude of group velocity by the polynomial in direction components, or one component of group velocity vector by polynomial in the remaining components; for example in the x_1x_3 -plane

$$v_G(\xi) = \sum_{j=1}^m a_j \xi^j, \text{ respectively, } (v_G)_3[(v_G)_1] = \sum_{j=1}^m b_j (v_G)_1^j \tag{11}$$

depending on the particular case.

Obviously, fitting the whole ray surface (or curve) by one polynomial cannot result in reliably reconstructed normal surface, especially when the fitted ray surface contains cuspidal regions. Hence the polynomial approximation has to be applied piecewise, fitting smooth regions separately by suitably connected local fits.

However, any other kind of analytical fitting can be employed, provided that the following conditions are satisfied:

1. In the principal crystallographic directions, where the group and phase velocity coincide, the fitting function has to be of zero derivative in all direction components.
2. The fitting function should not contain any inflections.

The idea of the first condition is obvious. By demanding the derivatives to be zero, the coincidence of input group velocity with reconstructed phase velocity is assured.

The second condition follows from the fact that the principle curvatures of the ray surfaces are naturally positive except of those surfaces containing cuspidal regions, where the sign of one of the second derivatives changes discontinuously at the edges of the cusp (the latter principle curvature must remain positive due to the rotational invariance about the x_3 -axis). When the cuts of these surfaces are to be geometrically converted into corresponding phase velocities, the fitted regions are, thus, always pure convex or concave. Possible inflections on fitting functions might result in an appearance of similar cuspidal regions on the reconstructed phase velocity surface, contrary to the nature of normal surfaces.

As it follows from the above proposed conditions, the high-order polynomials are unsuitable for ray surface fitting because of possible inflections contained. In Fig. 6, the importance of a choice of the fitting function is demonstrated by fitting the same group velocities by polynomials of different degrees m . All polynomial fits are in a similar good agreement with approximated data but the geometrically recovered normal surfaces significantly differ from each other. For $m = 4$, the fitting polynomial contains an inflection corresponding to cuspidal region on the normal surface.

The high-order polynomials might be useful only for piecewise fitting of evidently concave or convex ray surface regions, in which the data distortion cannot influence the character of the fit.

However, the piecewise fitting may have a consequence of discontinuities in the ray surface first derivatives and resultant discontinuities on recovered normal surfaces, especially when the input data are significantly distorted. Then the local fits must be smoothly connected to each other using e.g. a linear affine combination. For the fitted region divided equidistantly into intervals $\langle \xi_n; \xi_{n+1} \rangle$ the combined fitting function takes the form

$$[v_G(\xi)]_{\xi \in \langle \xi_n; \xi_{n+1} \rangle} = v_n \sum_{i=0}^{m_a} a_i \xi^i + (1 - v_n) \sum_{i=0}^{m_b} b_i \xi^i, \quad (12)$$

where the monotone linear sequences $\{v_n\}_1^N = \{\frac{1}{N}, \frac{2}{N}, \dots, \frac{N-1}{N}, 1\}$ represent the share of the first poly-

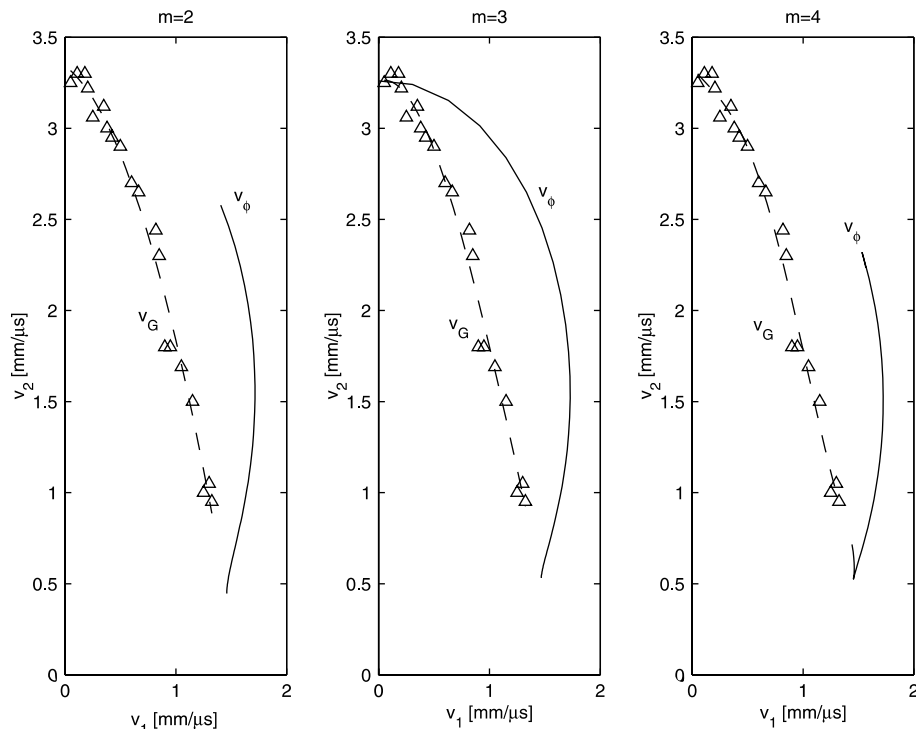


Fig. 6. Importance of a choice of the fitting function.

mial $\sum_{i=0}^{m_a} a_i \zeta^i$ to the whole fitting function. The share of the second polynomial $\sum_{i=0}^{m_b} b_i \zeta^i$ is equal the the affine complement series $1 - v_n$. In each interval, the value of v_n is treated as constant.

When the connected polynomials differ significantly in their magnitudes or derivatives, ‘smoother’ forms of affine combinations can be utilized, such as

$$[v_G(\xi)]_{\xi \in \langle \xi; \xi_{n+1} \rangle} = \sin^2\left(\frac{\pi}{2} v_n\right) \sum_{i=0}^{m_a} a_i \zeta^i + \cos^2\left(\frac{\pi}{2} v_n\right) \sum_{i=0}^{m_b} b_i \zeta^i, \tag{13}$$

which reduces the share of the second polynomial in the first interval $\langle \xi_1; \xi_2 \rangle$ from $\frac{1}{N}$ to $\sin^2(\frac{1}{N})$, and the share of the first polynomial in the last interval similarly.

Due to the linearity of derivatives, the tangents and normals to this function in each interval can be evaluated from similar affine combinations of first-order derivatives. Resulting fits are then smoother and the probability of discontinuity occurrence on recovered normal surface is minimized, see Fig. 7. In the Fig. 7a, a quadrant of group velocities (triangles) is fitted by two second-order polynomials (dashed line), each satisfying one of the extremal conditions in principal directions x_1 and x_3 . The fit is continuous and close to smooth but an imperceptible jump in the first derivative (see the arrow) results in significant discontinuity on the recovered normal surface. When connecting both polynomials together via affine combinations (12) or (13), respectively, the discontinuity disappears, as demonstrated for the affine combination (13) in Fig. 7b, where

the thick lines denote the regions both on the ray and on the normal surface where the affine combination has been applied. For affine combination (12), the result will be very similar.

Stability of the optimization process versus type and reliability of group velocity fitting is a complex problem, that cannot be illustratively simulated as it was done for distortion and incompleteness of phase velocities.

The distortion of input group velocity data may either be eliminated by smooth fitting or result in normal surface completely unapplicable for ensuing inverse computation.

Similar extensive simulation as for phase velocities was performed to outline the dependence of output elastic coefficients on input group velocity distortion. Thirty sets of randomly distorted group velocities (normal distribution considered) were piecewise fitted using both the affine combinations (12) and (13) of 4th order polynomials.

In contrast to previous simulations, the geometrical conversion influences the optimization results systematically. As listed in Table 4, the average values of coefficients c_{13} and c_{33} differ more than negligibly from correct values. Whereas the coefficients c_{33} are of comparable inaccuracies, for the coefficient c_{13} the affine combination (13) seems to be more suitable.

The corresponding relative standard deviations are listed in Table 5.

Surprisingly, the resultant distortion of optimized coefficients c_{ij} is very close to standard deviations

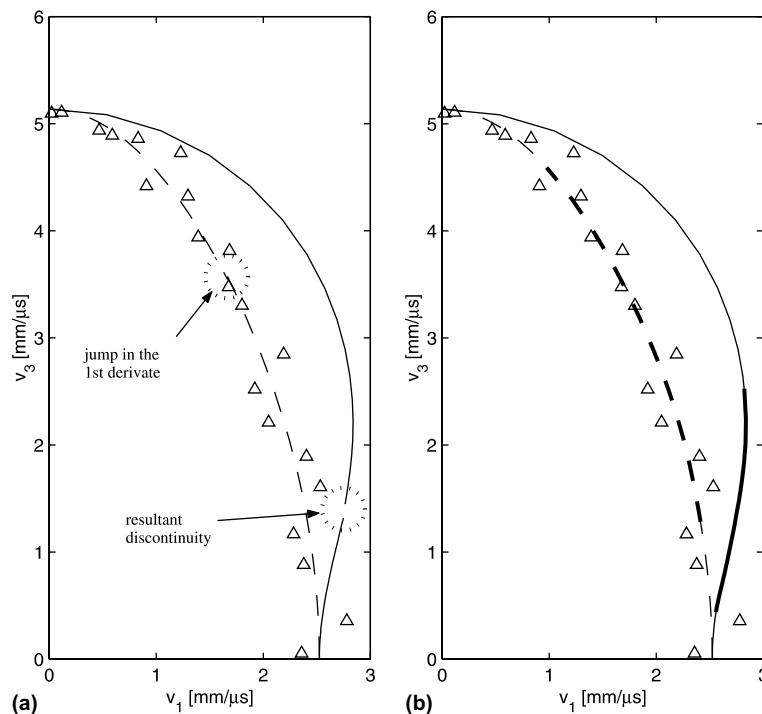


Fig. 7. Difference between the usage of: (a) piecewise polynomial fitting and (b) the connection of fitting functions by affine combination (13).

Table 4

Differences δ_{ij} between average output and correct values c_{ij} of elastic coefficients after geometrical conversion of group velocities

Distortion	Affine combination (12)		Affine combination (13)	
	δ_{13} (%)	δ_{33} (%)	δ_{13} (%)	δ_{33} (%)
1	4.85	0.01	4.56	0.08
2	2.65	0.37	3.01	0.31
3	17.23	0.07	6.90	0.30

Table 5

Relative standard deviations of output values of c_{ij} after geometrical conversion of group velocities

Distortion (%)	Affine combination (12) (%)		Affine combination (13) (%)	
	SD _{13/c₁₃} (%)	SD _{33/c₃₃} (%)	SD _{13/c₁₃} (%)	SD _{33/c₃₃} (%)
1	9.14	0.82	7.27	0.67
2	16.62	1.59	15.34	1.80
3	38.20	2.45	28.10	2.16

obtained from simulating the stability of inversion from phase velocities. It can be thus concluded, that the geometrical conversion into phase velocities does not, in general, amplify the effect of input data distortion. Similar conclusions have recently been published by Detg-yar and Rokhlin [24] for inverse determination of anisotropic elastic coefficients by two-step iterative method [2,7,25].

Concisely, the values of c_{ij} optimized from the set of group velocities can be expressed as

$$c_{ij}^{\text{output}} = c_{ij}^{\text{exact}}(1 + \delta_{ij}) \pm \text{SD}_{ij}, \quad (14)$$

where the systematic deviation of the average value δ_{ij} results from the geometrical conversion and the source of accidental inaccuracies SD_{ij} should be sought in input data distortion.

The group velocity data incompleteness is expected to influence the optimization results similarly as the incompleteness of phase velocities. Although it must be taken into account that the corresponding regions on the normal and ray surface can be disproportional to each other. Large segments of normal surface can correspond to inconsiderable segments of ray surface and vice versa. The conclusion on the effect of data incompleteness must always be applied to converted phase velocities.

7. Concluding remarks

In this paper, the inverse algorithm for the determination of elastic coefficients of transversely isotropic solids based on simplex minimization of the difference between experimental and computed values was analyzed. Main possible sources of algorithm instabilities were briefly outlined a their effect on resultant optimized elastic properties was demonstrated by extensive simulations. From these simulations it was concluded that the input data distortion did not in general significantly destabilize the discussed inverse process, whereas the omission

of one of propagation modes might result in quite incorrect optimized values. It remains to be discussed how are the optimization results systematically influenced by the technique used for the determination of the wave arrivals on the detectors.

The information about particular elastic coefficients was revealed as inhomogenously distributed along the normal surface. The precisely accurate measurements of phase or group velocities may thus be not sufficient for stable optimization if they do not cover appropriate segments of normal or ray surfaces.

The conditions on reliable geometrical conversion of group velocities into corresponding phase velocities was discussed, especially with respect to the choice of the fitting function. Principal conditions for such fitting functions were postulated, as they followed from the natural symmetry and pure convexity/concavity of ray surfaces. Additional simulations were performed to illustrate that the geometrical conversion did not need to result in significant loss of optimized data correctness, provided that the fitting function was chosen sensitively.

The disadvantages of high-order polynomial fitting of group velocities for the geometrical conversion was pointed out, compared to more suitable lower-order piecewise polynomial fitting, employing affine combinations to smoothly connect the fitting polynomials to each other.

Numerical results of all simulations in this study are naturally relevant only to the particular examined material or for materials with very close mechanical properties. However, the approach of the above analysis and general conclusions are applicable to any other kind of materials.

Acknowledgment

This work was supported by the Grant Agency of the Academy of Sciences of the Czech Republic under pro-

ject No. IBS2076356 and the Institutional project AVOZ2076919.

The authors wish to express their thanks to Dr. J. Plešek for critical reading the manuscript and for fruitful comments.

References

- [1] A.G. Every, W. Sachse, *Dynamic Methods for measuring the elastic properties of solids Handbook of Elastic Properties of Solids, Liquids and Gases*, vol. I, Academic Press, San Diego, 2001.
- [2] T.-T. Wu, Z.-H. Ho, *Exper. Mech.* 30 (1990) 313–318.
- [3] S. Baudouin, B. Hosten, *J. Acoust. Soc. Am.* 102 (1997) 3450–3457.
- [4] S.I. Rokhlin, W. Wang, *J. Acoust. Soc. Am.* 91 (1992) 3303–3312.
- [5] Y.C. Chu, S.I. Rokhlin, *J. Acoust. Soc. Am.* 96 (1994) 342–352.
- [6] K. Balasubramaniam, S.C. Whitney, *NDT&E Int.* 29 (1996) 225–236.
- [7] A.G. Every, W. Sachse, *Phys. Rev. B* 42 (1990) 8196–8205.
- [8] W. Sachse, K.Y. Kim, N.N. Hsu, *Characterizing homogeneous, anisotropic elastic media*, in: A. Wirgin (Ed.), *Identification of Media and Structures by Inversion of Mechanical Wave Propagation*, Proceedings of CISM course (398), Udine, Italy, July 1998.
- [9] K.Y. Kim, W. Sachse, *Phys. Rev. B* 47 (1993) 10993–11000.
- [10] K.Y. Kim, R. Sribar, W. Sachse, *J. Appl. Phys.* 77 (1995) 5589–5600.
- [11] B. Audoin, *Ultrasonics* 40 (2002) 736–740.
- [12] H. Seiner, M. Landa, in: M. Černý (Ed.), *International Symposium on Mechanics of Composites*, Prague 2002, pp. 129–136.
- [13] H. Seiner, M. Landa, *Acta Tech. CSAV* 47 (2002) 400–418.
- [14] M.J.P. Musgrave, *Crystal Acoustics*, Holden-Day, San Francisco, 1970.
- [15] B.A. Auld *Acoustic Fields and Waves Solids*, vol. 1, John Wiley and Sons, New York, 1973.
- [16] K. Helbig, *Foundations of Anisotropy for Exploration Seismics*, Pergamon Press, Oxford, 1994.
- [17] R.F.S. Hearmon, *Introduction to Applied Anisotropic Elasticity*, Oxford University Press, 1961.
- [18] K.Y. Kim, *Phys. Rev. B* 49 (1994) 3713–3724.
- [19] W.H. Press, S.A. Teukolsky, W.T. Vetterling, B.P. Flannery, *Numerical Recipes in C*, Cambridge University Press, Cambridge, 1992.
- [20] P. Lasaygues, M. Pithioux, *Ultrasonics* 39 (2002) 567–573.
- [21] A.G. Every, W. Sachse, *Ultrasonics* 30 (1992) 43–48.
- [22] Y.C. Chu, S.I. Rokhlin, *J. Acoust. Soc. Am.* 96 (1994) 213–225.
- [23] A. Minachi, D.K. Hsu, R.B. Thompson, *J. Acoust. Soc. Am.* 96 (1994) 353–362.
- [24] A.D. Degtyar, S.I. Rokhlin, *J. Acoust. Soc. Am.* 102 (1997) 3458–3466.
- [25] M. Deschamps, C. Bescond, *Ultrasonics* 33 (1995) 205–211.